Research Article

Shao-Wen Yao, Talat Korpinar, Dumitru Baleanu, Zeliha Korpinar, Bandar Almohsen, and Mustafa Inc*

Magnetic charged particles of optical spherical antiferromagnetic model with fractional system

https://doi.org/10.1515/phys-2021-0047
received December 30, 2020; accepted May 25, 2021

Abstract: In this article, we first consider approach of optical spherical magnetic antiferromagnetic model for spherical magnetic flows of ϒ-magnetic particle with spherical de-Sitter frame in the de-Sitter space $\mathbb{S}_1^2$. Hence, we establish new relationship between magnetic total phases and spherical timelike flows in de-Sitter space $\mathbb{S}_1^2$. In other words, the applied geometric characterization for the optical magnetic spherical antiferromagnetic spin is performed. Moreover, this approach is very useful to analyze some geometrical and physical classifications belonging to ϒ-particle. Besides, solutions of fractional optical systems are recognized for submitted geometrical designs. Geometrical presentations for fractional solutions are obtained to interpret the model. These obtained results represent that operation is a compatible and significant application to restore optical solutions of some fractional systems. Components of models are described by physical assertions with solutions. Additionally, we get solutions of optical fractional flow equations with designs of our results in de-Sitter space $\mathbb{S}_1^2$.

*** Corresponding author: Mustafa Inc,** Department of Computer Engineering, Biruni University, Istanbul, Turkey; Department of Mathematics, Fırat University, Science Faculty, 23119, Elazığ, Turkey; Department of Medical Research, China Medical University, Taichung, Taiwan, e-mail: minc@firat.edu.tr
Shao-Wen Yao: School of Mathematics and Information Science, Henan Polytechnic University, Jiaozuo 454000, China
Talat Korpinar: Department of Mathematics, Mus Alparslan University, 49250, Mus, Turkey
Dumitru Baleanu: Department of Mathematics, Cankaya University, Balgat 06530, Ankara, Turkey; Institute of Space Sciences, Magurele-Bucharest R76900, Romania, e-mail: dumitru@cankaya.edu.tr
Zeliha Korpinar: Department of Administration, Mus Alparslan University, Mus, Turkey
Bandar Almohsen: Department of Mathematics, College of Science, King Saud University, P.O. Box 2455, Riyadh 11451, Saudi Arabia

Keywords: ϒ-magnetic particle, geometric phase, optical fiber, evolution equations, traveling wave hypothesis, antiferromagnetic

1 Introduction

Recently, improvement of optical lasers with the application of optical magnetic fiber operators has observed immense influence on spherical propagation by fluid flows. The complete torque density of the optical phase with magnetic light anholonomy has been characterized by considering geometrical fibers. Its construction and effect have been reported as either dynamic or systematic. Smith [1] investigated the phase of distinction of light propagating along with the monochromatic geometric fiber in which it is established by electromagnetic fields with spherical particle flows in a spherical fiber generator. Also, elementary verification of optical effect of phase of magnetic geometric light propagating in optical fiber was expanded [2]. Ross revised an exactly optical system to review rotation in coiled geometrical fiber with a fixed density and confirmed it is generated with diverse evaluations in fiber edge into geometric fibers. Tomita and Chiao [3] constructed a review of fiber optical shapes. Hence, Chiao and Wu [4] received an advanced essential optical phase of results for geometric density. Further leading research [6–10], we introduce diverse electromagnetic optical phase by antiferromagnetic model.

The optical phase is principally inspected by new electromagnetic phases and their advertiser. Optical nonlinear flow models are regularly executed as construction to determine considerably involved optical advancements in distinct functions of ferromagnetic models, principally in chemical physics, genuine-state physics, plasma physics, fluid mechanics, optical applied physics, etc. [11–23].

It is remarkable that in numerous fields of physics, the utilizations of approximately wave interpretation and its reactions are of comprehensive importance. The improvements of the natural traveling wave solutions are natural consequences of the selection of some representative variety related to some partial differential and nonlinear fractional differential equations (FDEs). Thus, flood waves are commonly immensely significant of all-instinctive phenomena; they have a superordinary elegant mathematical construction.

The fractional optical theory is a remarkably extensive, momentous of physics, mathematics, and engineering that plays a distinguished segment in an immense scope of consideration in some scientific areas. Fractional geometry perturbs the operations of derivatives and integrals of optional order. Over the latest several decades, enormous recognition because of its numerous modeling in distinct scientific competitions has been obtained. Arbitrary-order designs are softer integer-order designs. FDEs appear in various mathematical and modeling regions comparatively physics, geophysics, polymer rheology, biophysics, capacitor theory, aerodynamics, medicine, nonlinear vibration of earthquake, supervision theory, vital fluid flow phenomena, superelasticity, and magnetical districts. For the intensive study of its utilization, we introduce some comprehensive works [24–28].

Methodologies of fractional theory have been strongly managed in modeling some real elements in optical physics. Also, fractional differential systems are found to be a superb apparatus to define certain optical phenomena along with diffusion processes, damping laws, electrostatics, electrodynamics, elasticity, fluid flow, and various others [29–37].

Also, there is an immediately growing significance in finding a valuable and reliable applied modeling technique for some equations. Thus, this method has been successfully implemented for handling different physics phenomena including optics, atomic and nuclear physics, plasma, and other sections in optical physics and mathematical physics [38–42]. Then, some optical and approximate solution designs and their descriptive applications have been described in refs [43–45].

The aim of our work, that is, a general development method is recommended for spherical magnetic total phase and new solutions of fractional flow equations with illustrations of results in de Sitter space $\mathbb{S}_1^2$. We consider the cases of magnetic antiferromagnetic spin for Lorentz forces. The advantage of our used technique on other methods is that: we couple both theory of complex geometry of particles and antiferromagnetic theory and recover a special class of fractional flow equations. The applications of these models are magnetic surfaces.

The outline of the article is constructed as follows. First, we consider approaches of optical spherical magnetic antiferromagnetic model for spherical magnetic flows of Υ-magnetic particle with spherical de-Sitter frame in the de-Sitter space $\mathbb{S}_1^2$. Hence, we establish new relationship between magnetic total phases and spherical timelike flows in de Sitter space $\mathbb{S}_1^2$. In other words, the applied geometric characterization for the optical magnetic spherical antiferromagnetic spin is performed. This approach further boosts analysis of some geometrical and physical classifications belonging to Υ-magnetic particle. Besides, solutions of fractional optical systems are recognized for submitted geometrical designs. Geometrical presentations for fractional solutions are performed to interpret the model. These obtained results represent that operation is a compatible and significant application to restore optical solutions of some fractional systems. Components of models are described by physical assertions with solutions. Additionally, we get solutions of optical fractional flow equations with designs of our results in de-Sitter space $\mathbb{S}_1^2$.

2 Spherical timelike Υ-magnetic particles in $\mathbb{S}_1^2$

In this section, the orthonormal frame design is explained by the orthonormal Lorentzian new spherical Sitter frame and the particle $\Upsilon : \mathbb{I} \to \mathbb{S}_1^2$ refreshing this spherical Sitter frame equation is defined by

$$\begin{bmatrix} \nabla_\sigma \Upsilon \\ \nabla_\sigma \mathbf{T} \\ \nabla_\sigma \mathbf{N} \end{bmatrix} = \begin{bmatrix} 0 & 1 & 0 \\ 1 & 0 & \varsigma \\ 0 & \varsigma & 0 \end{bmatrix} \begin{bmatrix} \Upsilon \\ \mathbf{T} \\ \mathbf{N} \end{bmatrix},$$

where ∇ is a Levi-Civita form and $\varsigma = \det(\Upsilon, \mathbf{T}, \nabla_\sigma \mathbf{T})$ is the curvature of particle [19]]. Then products of spherical vector fields are presented by

$$\Upsilon = \mathbf{T} \wedge \mathbf{n}, \quad \mathbf{t} = \Upsilon \wedge \mathbf{n}, \quad \mathbf{n} = \Upsilon \wedge \mathbf{T}.$$

Assume that $\Upsilon : I \to \mathbb{S}_1^2$ be a timelike spherical Υ-magnetic particle and $\mathcal{G}$ be the magnetic field in $\mathbb{S}_1^2$. Timelike spherical Υ-magnetic particle is defined by

$$\nabla_\sigma \Upsilon = \phi(\Upsilon) = \mathcal{G} \times \Upsilon.$$

$\star$ Lorentz force ϕ of Υ-magnetic particle with the magnetic field $\mathcal{G}$ is presented by

$$\begin{aligned} \phi(\Upsilon) &= \mathbf{T}, \\ \phi(\mathbf{T}) &= \Upsilon + \pi_1 \mathbf{N}, \\ \phi(\mathbf{N}) &= \pi_1 \mathbf{T}, \\ \mathcal{G}^{\Upsilon} &= \pi_1 \Upsilon - \mathbf{N}, \end{aligned}$$

where $\pi_1 = h(\phi(\mathbf{T}), \mathbf{N})$.

Let $\Upsilon(s,t)$ be the evolution of Υ-magnetic particle in de Sitter space. Flow of Υ-magnetic particle is given by

$$\nabla_t\Upsilon = \chi_1\mathbf{T} + \chi_2\mathbf{N},$$

where χ_1, χ_2 are potentials.

First, we have

$$\nabla_\sigma\nabla_t\Upsilon = \chi_1\Upsilon + \left(\chi_2\varsigma + \frac{\partial\chi_1}{\partial\sigma}\right)\mathbf{T} + \left(\frac{\partial\chi_2}{\partial\sigma} + \chi_1\varsigma\right)\mathbf{N}.$$

⋆ Condition of Lorentz forces $\phi(\Upsilon)$, $\phi(\mathbf{T})$, $\phi(\mathbf{N})$ and magnetic field $\mathcal{G}^\Upsilon$ for rotational equilibrium of the timelike Υ-magnetic particle

$$\nabla_t\phi(\Upsilon) = \chi_1\Upsilon + \left(\frac{\partial\chi_2}{\partial\sigma} + \chi_1\varsigma\right)\mathbf{N},$$

$$\nabla_t\phi(\mathbf{T}) = -\pi_1\chi_2\Upsilon + \left(\chi_1 + \pi_1\left(\frac{\partial\chi_2}{\partial\sigma} + \varsigma\chi_1\right)\right)\mathbf{T} + \left(\frac{\partial\pi_1}{\partial t} + \chi_2\right)\mathbf{N},$$

$$\nabla_t\phi(\mathbf{N}) = \chi_1\pi_1\Upsilon + \frac{\partial}{\partial t}\pi_1\mathbf{T} + \left(\frac{\partial\chi_2}{\partial\sigma} + \chi_1\varsigma\right)\pi_1\mathbf{N},$$

$$\nabla_t\mathcal{G}^\Upsilon = \left(\frac{\partial\pi_1}{\partial t} + \chi_2\right)\Upsilon + \left(\pi_1\chi_1 - \left(\frac{\partial\chi_2}{\partial\sigma} + \chi_1\varsigma\right)\right)\mathbf{T} + \pi_1\chi_2\mathbf{N},$$

where $\pi_1 = h(\phi(\mathbf{T}), \mathbf{N})$.

By this way, the equation for Lorentz forces $\phi(\Upsilon)$, $\phi(\mathbf{T})$, $\phi(\mathbf{N})$ reads

$$\nabla_\sigma\phi(\Upsilon) = \Upsilon + \varsigma\mathbf{N},$$

$$\nabla_\sigma\phi(\mathbf{T}) = (\varsigma\pi_1 + 1)\mathbf{T} + \frac{\partial\pi_1}{\partial\sigma}\mathbf{N},$$

$$\nabla_\sigma\phi(\mathbf{N}) = \pi_1\Upsilon + \frac{\partial\pi_1}{\partial\sigma}\mathbf{T} + \varsigma\pi_1\mathbf{N},$$

$$\nabla_\sigma\mathcal{G}^\Upsilon = \frac{\partial}{\partial\sigma}\pi_1\Upsilon + (\pi_1 - \varsigma)\mathbf{T}.$$

3 New geometric results with physical applications

3.1 Magnetic antiferromagnetic spin for $\phi(\Upsilon)$

Definition of magnetic antiferromagnetic spin is given by

$$\nabla_t\phi(\Upsilon) = \phi(\Upsilon) \times \nabla_\sigma\phi(\Upsilon).$$

Then, it is easy to see that

$$\chi_1 = \varsigma,$$

$$\frac{\partial\chi_2}{\partial\sigma} + \chi_1\varsigma = -1.$$

Magnetic total phase along Lorentz force $\phi(\Upsilon)$ is indicated by

$$\Phi^{\mathcal{G}^\Upsilon}_{\phi(\Upsilon)} = \int\int \phi(\Upsilon)\cdot \mathcal{G}^\Upsilon \times \nabla_t\phi(\Upsilon)\mathrm{d}\varrho.$$

With some calculations, we have

$$\mathcal{G}^\Upsilon \times \nabla_t\phi(\Upsilon) = \left(\pi_1\left(\frac{\partial\chi_2}{\partial\sigma} + \varsigma\chi_1\right) + \chi_1\right)\mathbf{T}.$$

Magnetic anholonomy density for $\phi(\Upsilon)$ is

$$\rho^{\mathcal{G}^\Upsilon}_{\phi(\Upsilon)} = -\left(\pi_1\left(\frac{\partial\chi_2}{\partial\sigma} + \chi_1\varsigma\right) + \chi_1\right).$$

Also, we present

$$\Phi_{\phi(\Upsilon)} = -\int\int\left(\left(\pi_1\left(\frac{\partial\chi_2}{\partial\sigma} + \chi_1\varsigma\right) + \chi_1\right)\right)\mathrm{d}\varrho.$$

From magnetic spherical anholonomy density with antiferromagnetic model is obtained

$$^{\mathcal{AFR}}\rho^{\mathcal{G}^\Upsilon}_{\phi(\Upsilon)} = \phi(\Upsilon)\cdot \mathcal{G}^\Upsilon \times \phi(\Upsilon) \times \nabla_\sigma\phi(\Upsilon).$$

By this way, we conclude

$$^{\mathcal{AFR}}\rho^{\mathcal{G}^\Upsilon}_{\phi(\Upsilon)} = -(\varsigma - \pi_1).$$

Similarly, we can easily obtain that

$$^{\mathcal{AFR}}\Phi^{\mathcal{G}^\Upsilon}_{\phi(\Upsilon)} = -\int\int(\varsigma - \pi_1)\mathrm{d}\varrho.$$

Spherical magnetic anholonomy density and timelike Υ-magnetic particle flow in a kernel of magnetic quadrupole for timelike spherical evolution with $\phi(\Upsilon)$. Spherical antiferromagnetic density is illustrated with antiferromagnetic density design in Figure 1.

3.2 Magnetic antiferromagnetic spin for $\phi(\mathbf{T})$

Magnetic antiferromagnetic spin is presented by

$$\nabla_t\phi(\mathbf{T}) = \phi(\mathbf{T}) \times \nabla_\sigma\phi(\mathbf{T}).$$

First,

$$\nabla_\sigma\phi(\mathbf{T}) = (1 + \pi_1\varsigma)\mathbf{T} + \frac{\partial\pi_1}{\partial\sigma}\mathbf{N},$$

and thus we obtain

$$\phi(\mathbf{T}) \times \nabla_\sigma\phi(\mathbf{T}) = -\pi_1(1 + \pi_1\varsigma)\Upsilon + \frac{\partial\pi_1}{\partial\sigma}\mathbf{T}(1 + \pi_1\varsigma)\mathbf{N}.$$

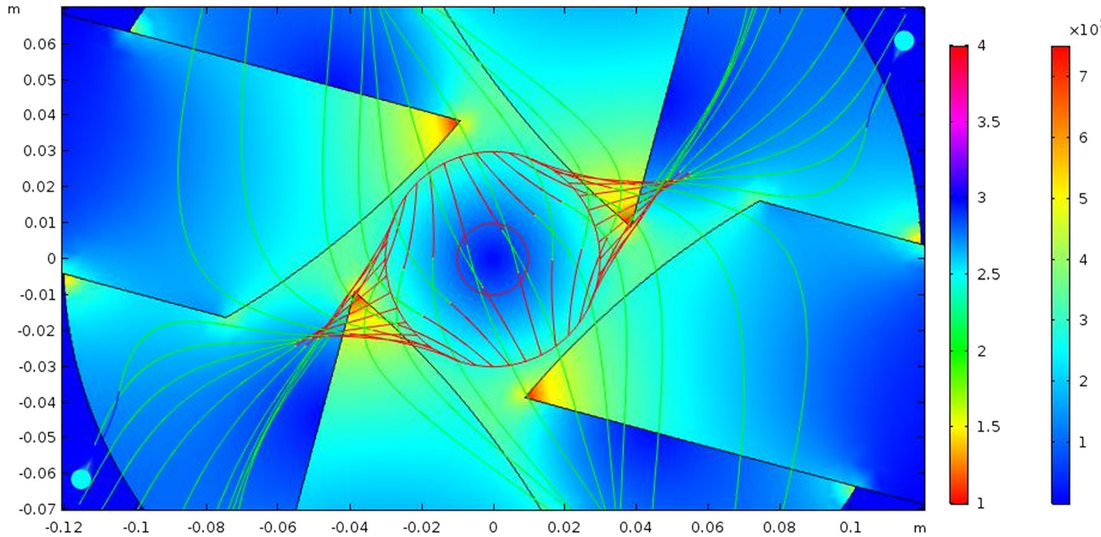

Figure 1: Spherical antiferromagnetic density with $\phi(\Upsilon)$.

Also, from time parameter, we get

$$\nabla_t \phi(\mathbf{T}) = -\pi_1\chi_2\Upsilon + \left(\chi_1 + \pi_1\left(\frac{\partial\chi_2}{\partial\sigma} + \chi_1\varsigma\right)\right)\mathbf{T} + \left(\frac{\partial\pi_1}{\partial t} + \chi_2\right)\mathbf{N}.$$

Continuing,

$$\begin{aligned}\chi_2 &= (1 + \pi_1\varsigma),\\ \frac{\partial\pi_1}{\partial\sigma} &= \chi_1 + \pi_1\left(\frac{\partial\chi_2}{\partial\sigma} + \chi_1\varsigma\right),\\ -(1 + \pi_1\varsigma) &= \frac{\partial\pi_1}{\partial t} + \chi_2,\end{aligned}$$

which

$$\begin{aligned}\chi_2 &= (1 + \pi_1\varsigma),\\ \frac{\partial\pi_1}{\partial\sigma} &= \chi_1 + \pi_1\left(\frac{\partial\chi_2}{\partial\sigma} + \chi_1\varsigma\right),\\ -2\chi_2 &= \frac{\partial\pi_1}{\partial t}.\end{aligned}$$

Magnetic total spherical phase of force $\phi(\mathbf{T})$ is obtained by

$$\Phi^{\mathcal{G}^{\Upsilon}}_{\phi(\mathbf{T})} = \int\int \phi(\mathbf{T})\cdot \mathcal{G}^{\Upsilon} \times \nabla_t\phi(\mathbf{T})d\varrho.$$

Since, we express

$$\begin{aligned}\mathcal{G}^{\Upsilon} \times \nabla_t\Upsilon(\mathbf{T}) = &\left(\chi_1 + \pi_1\left(\frac{\partial\chi_2}{\partial\sigma} + \varsigma\chi_1\right)\right)\Upsilon\\ &+ \left(\pi_1\left(\frac{\partial\pi_1}{\partial t} + \chi_2\right) - \pi_1\chi_2\right)\mathbf{T}\\ &+ \pi_1\left(\chi_1 + \pi_1\left(\frac{\partial\chi_2}{\partial\sigma} + \chi_1\varsigma\right)\right)\mathbf{N}.\end{aligned}$$

Then

$$\rho^{\mathcal{G}^{\Upsilon}}_{\phi(\mathbf{T})} = \left(\chi_1 + \pi_1\left(\frac{\partial\chi_2}{\partial\sigma} + \chi_1\varsigma\right)\right) + \pi_1^2\left(\chi_1 + \pi_1\left(\frac{\partial\chi_2}{\partial\sigma} + \chi_1\varsigma\right)\right).$$

From magnetic total phase, we obtain

$$\begin{aligned}\Phi^{\mathcal{G}^{\Upsilon}}_{\phi(\mathbf{T})} = \int\int\Bigg(&\left(\chi_1 + \pi_1\left(\frac{\partial\chi_2}{\partial\sigma} + \chi_1\varsigma\right)\right)\\ &+ \pi_1^2\left(\chi_1 + \pi_1\left(\frac{\partial\chi_2}{\partial\sigma} + \chi_1\varsigma\right)\right)\Bigg)d\varrho.\end{aligned}$$

Using magnetic antiferromagnetic spin for $\phi(\mathbf{T})$, we have

$$^{\mathcal{AFR}}\rho^{\mathcal{G}^{\Upsilon}}_{\phi(\mathbf{T})} = \phi(\mathbf{T})\cdot \mathcal{G}^{\Upsilon} \times \phi(\mathbf{T}) \times \nabla_{\mathbf{t_q}}\phi(\mathbf{T}).$$

Since

$$^{\mathcal{AFR}}\rho^{\mathcal{G}^{\Upsilon}}_{\phi(\mathbf{T})} = \frac{\partial\pi_1}{\partial\sigma} - \pi_1^2\frac{\partial\pi_1}{\partial\sigma}.$$

Finally, magnetic total spherical phase can be indicated by

$$^{\mathcal{AFR}}\Phi^{\mathcal{G}^{\Upsilon}}_{\phi(\mathbf{T})} = \int\int\left(\frac{\partial\pi_1}{\partial\sigma} - \pi_1^2\frac{\partial\pi_1}{\partial\sigma}\right)d\varrho.$$

Spherical magnetic anholonomy density and timelike Υ-magnetic particle flows in kernel of magnetic quadrupole for timelike spherical evolution with $\phi(\mathbf{T})$. Spherical antiferromagnetic density is provided by antiferromagnetic density algorithm in Figure 2.

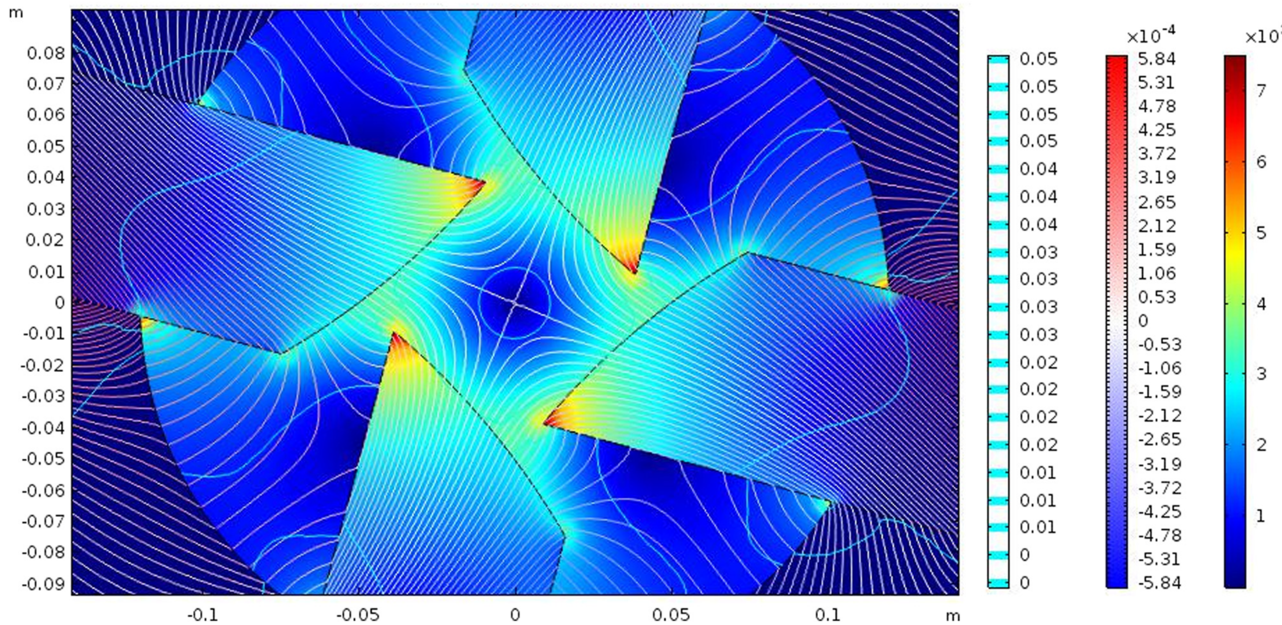

Figure 2: Spherical antiferromagnetic density with $\phi(\mathbf{T})$.

3.3 Magnetic antiferromagnetic spin for $\phi(\mathbf{N})$

From spherical Sitter frame, we get

$$\nabla_\sigma \phi(\mathbf{N}) = \pi_1 \Upsilon + \frac{\partial \pi_1}{\partial \sigma}\mathbf{T} + \varsigma \pi_1 \mathbf{N}.$$

Since

$$\phi(\mathbf{N}) \times \nabla_\sigma \phi(\mathbf{N}) = \frac{\partial \pi_1}{\partial \sigma}\Upsilon + (\pi_1^2 \varsigma + \pi_1)\mathbf{T} + \pi_1 \frac{\partial \pi_1}{\partial \sigma}\mathbf{N}.$$

We instantly calculate

$$\nabla_t \phi(\mathbf{N}) = \pi_1 \chi_1 \Upsilon + \frac{\partial}{\partial t}\pi_1 \mathbf{T} + \pi_1\left(\frac{\partial \chi_2}{\partial \sigma} + \chi_1 \varsigma\right)\mathbf{N},$$

and hence we have

$$\begin{aligned} \pi_1 \chi_1 &= \pi_1, \\ \frac{\partial}{\partial t}\pi_1 &= (\pi_1^2 \varsigma + \pi_1), \\ \pi_1\left(\frac{\partial \chi_2}{\partial \sigma} + \chi_1 \varsigma\right) &= \pi_1 \frac{\partial \pi_1}{\partial \sigma}, \end{aligned}$$

which satisfy

$$\begin{aligned} \chi_1 &= 1, \\ \frac{\partial \pi_1}{\partial t} &= (\pi_1^2 \varsigma + \pi_1), \\ \frac{\partial \chi_2}{\partial \sigma} + \varsigma &= \frac{\partial \pi_1}{\partial \sigma}. \end{aligned}$$

Magnetic total spherical phase for spherical Lorentz force $\phi(\mathbf{N})$ is presented by

$$\Phi_{\phi(\mathbf{N})}^{\mathcal{G}^\Upsilon} = \int\int \phi(\mathbf{N}) \cdot \mathcal{G}^\Upsilon \times \nabla_t \phi(\mathbf{N}) \mathrm{d}\varrho.$$

With cross product, we have

$$\mathcal{G}^\Upsilon \times \nabla_t \phi(\mathbf{N}) = \pi_1 \frac{\partial}{\partial t}\pi_1 \mathbf{N} + \pi_1^2\left(\frac{\partial \chi_2}{\partial \sigma} + \chi_1 \varsigma\right)\mathbf{T} + \pi_1 \chi_1 \mathbf{T} + \frac{\partial}{\partial t}\pi_1 \Upsilon.$$

The resulting magnetic anholonomy density:

$$\rho_{\phi(\mathbf{N})}^{\mathcal{G}^\Upsilon} = -\pi_1^3\left(\frac{\partial \chi_2}{\partial \sigma} + \chi_1 \varsigma\right).$$

Using magnetic density equation in phase, we get

$$\Phi_{\phi(\mathbf{N})}^{\mathcal{G}^\Upsilon} = -\int\int\left(\pi_1^3\left(\frac{\partial \chi_2}{\partial \sigma} + \chi_1 \varsigma\right)\right)\mathrm{d}\varrho.$$

By using spherical Sitter frame, we give

$$\mathcal{G}^\Upsilon \times \nabla_t \phi(\mathbf{N}) = (\pi_1^2 \varsigma + \pi_1)\Upsilon + (\pi_1^2 + 1)\frac{\partial \pi_1}{\partial \sigma}\mathbf{T} + \pi_1(\pi_1^2 \varsigma + \pi_1)\mathbf{N}.$$

Also,

$$^{\mathcal{AFR}}\rho_{\phi(\mathbf{N})}^{\mathcal{G}^\Upsilon} = -\pi_1(\pi_1^2 + 1)\frac{\partial \pi_1}{\partial \sigma}.$$

Since, we instantly arrive at

$$^{\mathcal{AFR}}\Phi_{\phi(\mathbf{N})}^{\mathcal{G}^\Upsilon} = \int\int\left(-\pi_1(\pi_1^2 + 1)\frac{\partial \pi_1}{\partial \sigma}\right)\mathrm{d}\varrho.$$

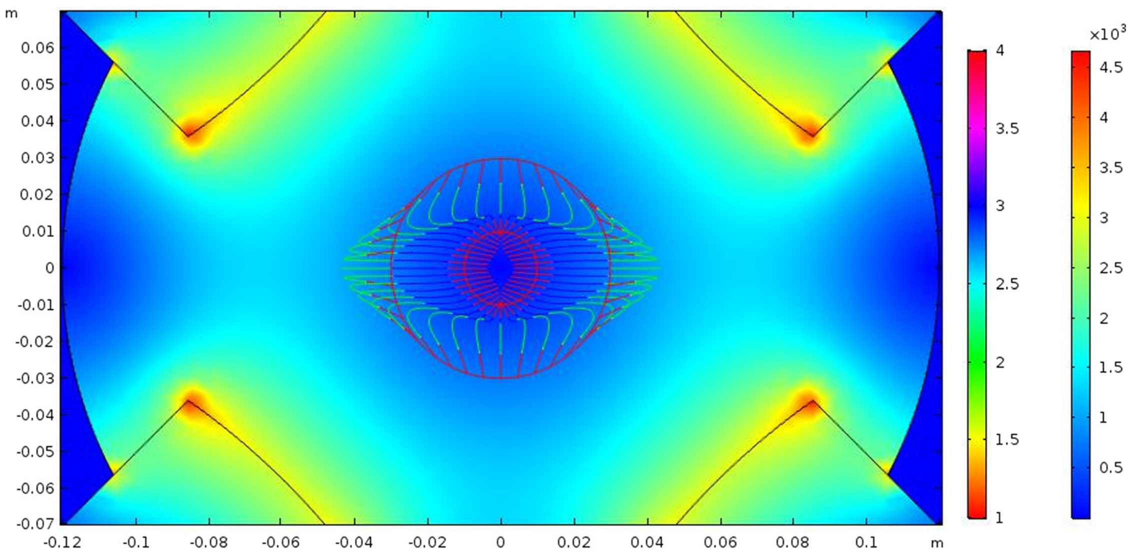

Figure 3: Spherical antiferromagnetic density with $\phi(\mathbf{N})$.

Spherical magnetic anholonomy density and timelike Υ-magnetic particle flows in kernel of magnetic quadrupole for timelike spherical evolution with Lorentz force $\phi(\mathbf{N})$. Spherical antiferromagnetic density is provided by antiferromagnetic density algorithm in Figure 3.

3.4 Antiferromagnetic spin for $\mathcal{G}^{\Upsilon}$

Magnetic antiferromagnetic spin is given by

$$\nabla_t \mathcal{G}^{\Upsilon} = \mathcal{G}^{\Upsilon} \times \nabla_\sigma \mathcal{G}^{\Upsilon}.$$

First,

$$\nabla_\sigma \mathcal{G}^{\Upsilon} = \frac{\partial \pi_1}{\partial \sigma}\Upsilon + (-\varsigma + \pi_1)\mathbf{T}.$$

It follows that

$$\mathcal{G}^{\Upsilon} \times \nabla_\sigma \mathcal{G}^{\Upsilon} = (\pi_1 - \varsigma)\Upsilon + \frac{\partial \pi_1}{\partial \sigma}\mathbf{T} - \pi_1(\pi_1 - \varsigma)\mathbf{N}.$$

Also,

$$\nabla_t \mathcal{G}^{\Upsilon} = \left(\frac{\partial \pi_1}{\partial t} + \chi_2\right)\Upsilon + \left(\pi_1\chi_1 - \left(\frac{\partial \chi_2}{\partial \sigma} + \varsigma\chi_1\right)\right)\mathbf{T} + \pi_1\chi_2\mathbf{N}.$$

By short estimation yields

$$\begin{aligned} \frac{\partial \pi_1}{\partial t} + \chi_2 &= \pi_1 - \varsigma, \\ \pi_1\chi_1 - \left(\frac{\partial \chi_2}{\partial \sigma} + \chi_1\varsigma\right) &= \frac{\partial}{\partial \sigma}\pi_1, \\ \chi_2 &= -(\pi_1 - \varsigma), \end{aligned}$$

So, one can have

$$\begin{aligned} \frac{\partial \pi_1}{\partial t} &= -2\chi_2, \\ \pi_1\chi_1 - \left(\frac{\partial \chi_2}{\partial \sigma} + \chi_1\varsigma\right) &= \frac{\partial}{\partial \sigma}\pi_1, \\ \chi_2 &= -(\pi_1 - \varsigma). \end{aligned}$$

Total phase is obtained by

$$\Phi_{\mathcal{G}^{\Upsilon}}^{\mathcal{G}^{\Upsilon}} = \int\int \mathcal{G}^{\Upsilon} \cdot \mathcal{G}^{\Upsilon} \times \nabla_t \mathcal{G}^{\Upsilon} d\varrho.$$

Since, we express

$$\begin{aligned} \mathcal{G}^{\Upsilon} \times \nabla_t \mathcal{G}^{\Upsilon} = &\left(\pi_1\chi_1 - \left(\frac{\partial \chi_2}{\partial \sigma} + \chi_1\varsigma\right)\right)\Upsilon \\ &+ \left(\pi_1^2\chi_2 + \left(\frac{\partial \pi_1}{\partial t} + \chi_2\right)\right)\mathbf{T} \\ &+ \pi_1\left(\pi_1\chi_1 - \left(\frac{\partial \chi_2}{\partial \sigma} + \chi_1\varsigma\right)\right)\mathbf{N}. \end{aligned}$$

Then

$$\rho_{\mathcal{G}^{\Upsilon}} = \pi_1\left(\pi_1\chi_1 - \left(\frac{\partial \chi_2}{\partial \sigma} + \chi_1\varsigma\right)\right) - \pi_1\left(\pi_1\chi_1 - \left(\frac{\partial \chi_2}{\partial \sigma} + \chi_1\varsigma\right)\right) = 0.$$

From phase, we obtain

$$\begin{aligned} \Phi_{\mathcal{G}^{\Upsilon}}^{\mathcal{G}^{\Upsilon}} = \int\int &\left(\pi_1(\pi_1 - \varsigma)\frac{\partial \pi_1}{\partial \sigma}\pi_1\chi_2 - \left(\frac{\partial \pi_1}{\partial \sigma}\left(\pi_1\chi_1 - \left(\frac{\partial \chi_2}{\partial \sigma} + \chi_1\varsigma\right)\right)\right.\right. \\ &\left.\left. - (\pi_1 - \varsigma)\left(\frac{\partial \pi_1}{\partial t} + \chi_2\right)\right)\right) d\varrho. \end{aligned}$$

By magnetic antiferromagnetic model, we get

$$^{\mathcal{AFR}}\rho^{\mathcal{G}^{\Upsilon}}_{\mathcal{G}^{\Upsilon}} = 0.$$

Finally, we reach

$$^{\mathcal{AFR}}\Phi^{\mathcal{G}^{\Upsilon}}_{\mathcal{G}^{\Upsilon}} = 0.$$

4 Optical soliton for extended direct algebraic method with fractional equation in $\mathbb{S}^2_1$

In this part, we design optical fractional solutions of nonlinear flow equation governing of solitons by magnetic fields of polarized light ray traveling in spherical fractional optical fiber. Traveling wave assumption concept is operated to gauge some analytical soliton solutions. Then numerical duplications are also contributed to complement the rational conclusion. Also, we deal with the following evolution equations of Lorentz force $\phi(\Upsilon)$.

$$\begin{aligned} &\pi_{1t}^{(\eta)} + 2\chi_2 = 0\\ &\pi_{1\sigma} - \pi_1\chi_{2\sigma} - \chi_1\chi_{2\sigma\sigma} = 0, \quad t > 0,\ 0 < \eta \le 1, \end{aligned} \tag{4.1}$$

where $\pi_{1t}^{(\eta)}$ is the conformable derivative operator ($\pi_1 = \pi_1(\sigma, t)$); χ_1 is a real valued any constant.

The conformable derivative of order $\eta \in (0, 1]$ is defined as the subsequent interpretation [29]

$$_tD^{\eta}\zeta(t) = \lim_{\vartheta\to 0}\frac{\zeta(t + \vartheta t^{1-\eta}) - \zeta(t)}{\vartheta},\ \ \zeta : (0, \infty) \to \mathbb{R}. \tag{4.2}$$

Some of the components of the conformable derivative can be seen in refs [29,30].

(a) $_tD^{\eta}t^{\alpha} = \alpha t^{\alpha-\eta}, \quad \forall\eta \in \mathbb{R}$,

(b) $_tD^{\eta}(\zeta\varpi) = \zeta_t D^{\eta}\varpi + \varpi_t D^{\eta}\zeta$,

(c) $_tD^{\eta}(\zeta o\varpi) = t^{1-\eta}\varpi'(t)\zeta'(\varpi(t))$,

(d) $_tD^{\eta}\left(\frac{\zeta}{\varpi}\right) = \frac{\varpi_t D^{\eta}\zeta - \zeta_t D^{\eta}\varpi}{\varpi^2}$.

It is absolutely smooth to perform with this fractional derivative. Lately, considerable papers have been constructed associated with conformable variety of fractional computations [30–35].

- Assume that the traveling wave variable is

$$\pi_1(\sigma, t) = u(\phi), \quad \phi = \sigma - Q\frac{t^{\eta}}{\eta}. \tag{4.3}$$

Thus, we have

$$B(u, u_{\phi}, u_{\phi\phi}, u_{\phi\phi\phi}, \ldots) = 0. \tag{4.4}$$

- Recognize solution of equation (4.4),

$$u(\phi) = \sum_{i=0}^{N}\alpha_i G^i(\phi), \tag{4.5}$$

where $a_n \neq 0$ and $G(\phi)$ can be expressed by

$$G'(\phi) = \ln(A)(\zeta G^2(\phi) + \varpi G(\phi) + h), \quad A \neq 0, 1, \tag{4.6}$$

where h, ϖ, ζ are arbitrary fixed.

By placing the aforementioned equations, we have

$$\begin{aligned} &\pi_1(\sigma, t) = u(\phi),\ \chi_2(\sigma, t) = v(\phi),\\ &2v(\phi) - Qu'(\phi) = 0,\\ &u'(\phi) - u(\phi)v'(\phi) - \chi_1 v''(\phi) = 0. \end{aligned} \tag{4.7}$$

The solutions of the aforementioned equation be a finite series as

$$u(\phi) = \sum_{j=0}^{N}\alpha_j G^j(\phi), \quad v(\phi) = \sum_{j=0}^{M}\beta_j G^j(\phi), \tag{4.8}$$

where $G(\phi)$ satisfies equation (4.6), $\phi = \sigma - Q\frac{t^{\eta}}{\eta}$ and α_j, β_j for $j = \overline{1, N}$.

Then, we put as follows:

$$\begin{aligned} &u(\phi) = \alpha_0 + \alpha_1 G(\phi),\\ &v(\phi) = \beta_0 + \beta_1 G(\phi) + \beta_2 G(\phi)^2, \end{aligned} \tag{4.9}$$

where $G(\phi)$ satisfied equation (4.6).

Also, solving the above system, we get

$$\begin{aligned} &\alpha_0 = -\frac{3}{2}\chi_1\varpi\ln(A), \quad \alpha_1 = -3\chi_1\zeta\ln(A),\\ &\beta_0 = \frac{6\zeta h}{\varpi^2 - 4\zeta h}, \quad \beta_1 = \frac{6\zeta\varpi}{\varpi^2 - 4\zeta h},\\ &\beta_2 = \frac{6\zeta^2}{\varpi^2 - 4\zeta h}, \quad Q = -\frac{4}{\chi_1(\varpi^2 - 4\zeta h)\ln(A)^2}. \end{aligned} \tag{4.10}$$

Solutions of equation (4.1) are presented by

(1) If $\varpi^2 - 4h\zeta < 0$ and $\zeta \neq 0$, then

$$\pi_{11}(\sigma, t) = -\frac{3}{2}\chi_1\varpi \ln(A) - 3\chi_1\zeta \ln(A)\left(-\frac{\varpi}{2\zeta} + \frac{\sqrt{-(\varpi^2 - 4h\zeta)}}{2\zeta}\tan_A\left(\frac{\sqrt{-(\varpi^2 - 4h\zeta)}}{2}\phi\right)\right),$$

$$\chi_{21}(\sigma, t) = \frac{6\zeta h}{\varpi^2 - 4\zeta h} + \frac{6\zeta\varpi}{\varpi^2 - 4\zeta h}\left(-\frac{\varpi}{2\zeta} + \frac{\sqrt{-(\varpi^2 - 4h\zeta)}}{2\zeta}\tan_A\left(\frac{\sqrt{-(\varpi^2 - 4h\zeta)}}{2}\phi\right)\right)$$
$$+ \frac{6f^2}{\varpi^2 - 4\zeta h}\left(-\frac{\varpi}{2\zeta} + \frac{\sqrt{-(\varpi^2 - 4h\zeta)}}{2\zeta}\tan_A\left(\frac{\sqrt{-(\varpi^2 - 4h\zeta)}}{2}\phi\right)\right)^2,$$

$$\chi_{12}(\sigma, t) = -\frac{3}{2}\chi_1\varpi \ln(A) - 3\chi_1\zeta \ln(A)\left(-\frac{\varpi}{2\zeta} + \frac{\sqrt{-(\varpi^2 - 4h\zeta)}}{2\zeta}\cot_A\left(\frac{\sqrt{-(\varpi^2 - 4h\zeta)}}{2}\phi\right)\right),$$

$$\kappa_{22}(\sigma, t) = \frac{6\zeta h}{\varpi^2 - 4\zeta h} + \frac{6\zeta\varpi}{\varpi^2 - 4\zeta h}\left(-\frac{\varpi}{2\zeta} + \frac{\sqrt{-(\varpi^2 - 4h\zeta)}}{2\zeta}\cot_A\left(\frac{\sqrt{-(\varpi^2 - 4h\zeta)}}{2}\phi\right)\right)$$
$$+ \frac{6\zeta^2}{\varpi^2 - 4\zeta h}\left(-\frac{\varpi}{2\zeta} + \frac{\sqrt{-(\varpi^2 - 4\zeta h)}}{2\zeta}\cot_A\left(\frac{\sqrt{-(\varpi^2 - 4\zeta h)}}{2}\phi\right)\right)^2.$$

(2) If $\varpi^2 - 4\zeta h > 0$ and $\zeta \neq 0$, then singular soliton and dark solutions are presented by

$$\pi_{13}(\sigma, t) = -\frac{3}{2}\chi_1\varpi \ln(A) - 3\chi_1\zeta \ln(A)\left(-\frac{\varpi}{2\zeta} + \frac{\sqrt{\varpi^2 - 4\zeta h}}{4\zeta}\left(\tanh_A\left(\frac{\sqrt{\varpi^2 - 4\zeta h}}{4}\phi\right) + \coth_A\left(\frac{\sqrt{\varpi^2 - 4\zeta h}}{4}\phi\right)\right)\right),$$

$$\chi_{23}(\sigma, t) = \frac{6fh}{\varpi^2 - 4\zeta h} + \frac{6\zeta\varpi}{\varpi^2 - 4\zeta h}\left(-\frac{\varpi}{2\zeta} + \frac{\sqrt{\varpi^2 - 4\zeta h}}{4\zeta}\left(\tanh_A\left(\frac{\sqrt{\varpi^2 - 4h\zeta}}{4}\phi\right) + \coth_A\left(\frac{\sqrt{\varpi^2 - 4\zeta h}}{4}\phi\right)\right)\right)$$
$$+ \frac{6\zeta^2}{\varpi^2 - 4\zeta h}\left(-\frac{\varpi}{2\zeta} + \frac{\sqrt{\varpi^2 - 4\zeta h}}{4\zeta}\left(\tanh_A\left(\frac{\sqrt{\varpi^2 - 4\zeta h}}{4}\phi\right) + \coth_A\left(\frac{\sqrt{\varpi^2 - 4\zeta h}}{4}\phi\right)\right)\right)^2.$$

(3) If $h\zeta > 0$ and $\varpi = 0$, then singular spherical periodic solutions are presented by

$$\pi_{14}(\sigma, t) = -\frac{3}{2}\chi_1\varpi \ln(A) - 3\chi_1\zeta \ln(A)\left(\sqrt{\frac{h}{\zeta}}(\tan_A(2\sqrt{h\zeta}\phi) \pm \sqrt{\Delta\Omega}\sec_A(2\sqrt{h\zeta}\phi))\right),$$

$$\chi_{24}(\sigma, t) = \frac{6\zeta h}{g^2 - 4\zeta h} + \frac{6\zeta\varpi}{g^2 - 4\zeta h}\left(\sqrt{\frac{h}{\zeta}}(\tan_A(2\sqrt{h\zeta}\phi) \pm \sqrt{\Delta\Omega}\sec_A(2\sqrt{h\zeta}\phi))\right)$$
$$+ \frac{6\zeta^2}{\varpi^2 - 4\zeta h}\left(\sqrt{\frac{h}{\zeta}}(\tan_A(2\sqrt{h\zeta}\phi) \pm \sqrt{\Delta\Omega}\sec_A(2\sqrt{h\zeta}\phi))\right)^2.$$

(4) If $h\zeta < 0$ and $\varpi = 0$, then dark, singular, bright spherical soliton solutions are presented by

$$\pi_{15}(\sigma, t) = -3\chi_1\zeta \ln(A)\left(\sqrt{-\frac{h}{\zeta}}(-\coth_A(2\sqrt{-h\zeta}\phi) \pm \sqrt{\Delta\Omega}\operatorname{csch}_A(2\sqrt{-h\zeta}\phi))\right),$$

$$\chi_{25}(\sigma, t) = -\frac{6\zeta h}{4\zeta h} - \frac{6f^2}{4\zeta h}\left(\sqrt{-\frac{h}{\zeta}}(-\coth_A(2\sqrt{-h\zeta}\phi) \pm \sqrt{\Delta\Omega}\operatorname{csch}_A(2\sqrt{-h\zeta}\phi))\right)^2.$$

(5) If $h = \zeta$ and $\varpi = 0$, then singular periodic spherical solutions are presented by

$$\pi_{16}(\sigma, t) = -3\chi_1\zeta\ln(A)\left(\frac{1}{2}\left(\tan_A\left(\frac{h}{2}\phi\right) - \cot_A\left(\frac{h}{2}\phi\right)\right)\right),$$

$$\chi_{26}(\sigma, t) = -\frac{6\zeta h}{4\zeta h} - \frac{6\zeta\varpi}{4\zeta h}\left(\frac{1}{2}\left(\tan_A\left(\frac{h}{2}\phi\right) - \cot_A\left(\frac{h}{2}\phi\right)\right)\right) - \frac{6\zeta^2}{4\zeta h}\left(\frac{1}{2}\left(\tan_A\left(\frac{h}{2}\phi\right) - \cot_A\left(\frac{h}{2}\phi\right)\right)\right)^2.$$

(6) If $h = -\zeta$ and $\varpi = 0$, then dark soliton and singular spherical solutions are presented by

$$\pi_{17}(\sigma, t) = -3\chi_1\zeta\ln(A)(-\tanh_A(h\phi)),$$

$$\chi_{27}(\sigma, t) = -\frac{6\zeta h}{4\zeta h} - \frac{6\zeta\varpi}{4\zeta h}(-\tanh_A(h\phi)) - \frac{6\zeta^2}{4\zeta h}(-\tanh_A(h\phi))^2.$$

(7) If $\varpi^2 = 4h\zeta$, then rational spherical solution is presented by

$$\pi_{18}(\sigma, t) = -\frac{3}{2}\chi_1\varpi\ln(A) - 3\chi_1\zeta\ln(A)\left(-2h\frac{\varpi\phi\ln(A) + 2}{g^2\phi\ln(A)}\right),$$

$$\chi_{28}(\sigma, t) = \frac{6\zeta h}{\varpi^2 - 4\zeta h} + \frac{6\zeta\varpi}{\varpi^2 - 4\zeta h}\left(-2h\frac{\varpi\phi\ln(A) + 2}{\varpi^2\phi\ln(A)}\right) + \frac{6\zeta^2}{\varpi^2 - 4\zeta h}\left(-2h\frac{\varpi\phi\ln(A) + 2}{\varpi^2\phi\ln(A)}\right)^2.$$

(8) If $\varpi = k$, $h = mk$ $(m \neq 0)$ and $\zeta \neq 0$, then rational spherical solution is presented by

$$\pi_{19}(\sigma, t) = -\frac{3}{2}\chi_1\varpi\ln(A) - 3\chi_1\zeta\ln(A)(A^{k\phi} - m),$$

$$\chi_{29}(\sigma, t) = \frac{6\zeta h}{\varpi^2 - 4\zeta h} + \frac{6\zeta\varpi}{\varpi^2 - 4\zeta h}(A^{k\phi} - m) + \frac{6\zeta^2}{\varpi^2 - 4\zeta h}(A^{k\phi} - m)^2.$$

(9) If $h = 0$ and $\varpi \neq 0$, then dark-like spherical solitons are presented by

$$\pi_{112}(\sigma, t) = -\frac{3}{2}\chi_1\varpi\ln(A) - 3\chi_1\zeta\ln(A)\left(-\frac{\Delta\varpi}{\zeta(\cosh_A(\varpi\phi) - \sinh_A(\varpi\phi) + \Delta)}\right),$$

$$\chi_{212}(\sigma, t) = \frac{6\zeta\varpi}{\varpi^2}\left(-\frac{\Delta\varpi}{\zeta(\cosh_A(\varpi\phi) - \sinh_A(\varpi\phi) + \Delta)}\right) + \frac{6\zeta^2}{\varpi^2}\left(-\frac{\Delta\varpi}{\zeta(\cosh_A(\varpi\phi) - \sinh_A(\varpi\phi) + \Delta)}\right)^2.$$

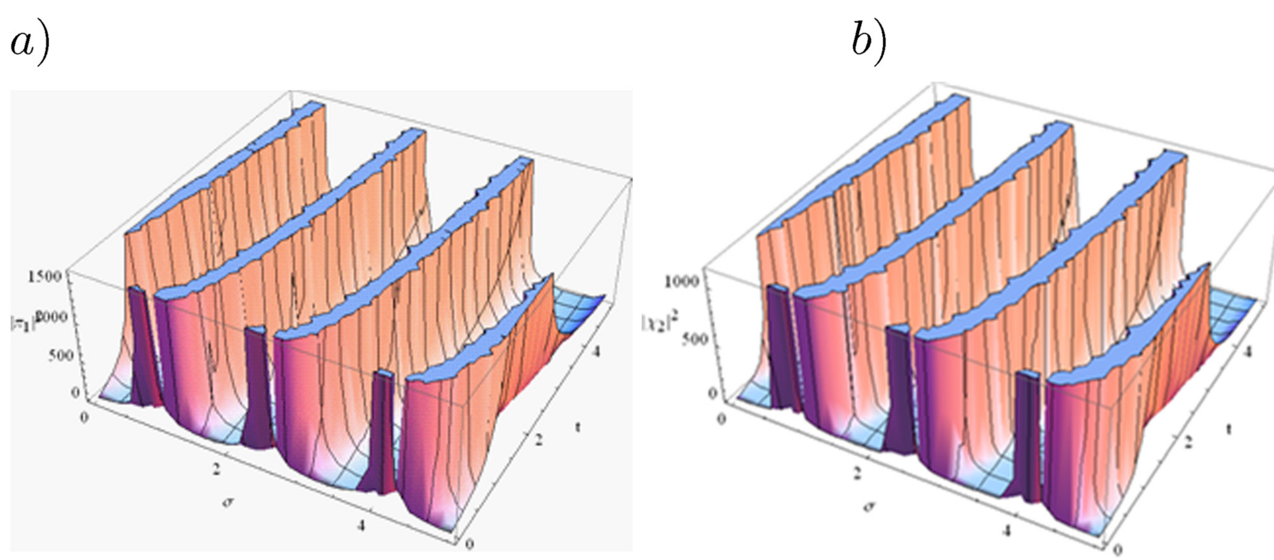

Figure 4: The magnetic flow graphics for the analytical solutions of the fractional (4.1) equations ($h = \zeta = 2$, $\varpi = 1$) (a) $\pi_{11}(\sigma, t)$, (b) $\chi_{21}(\sigma, t)$.

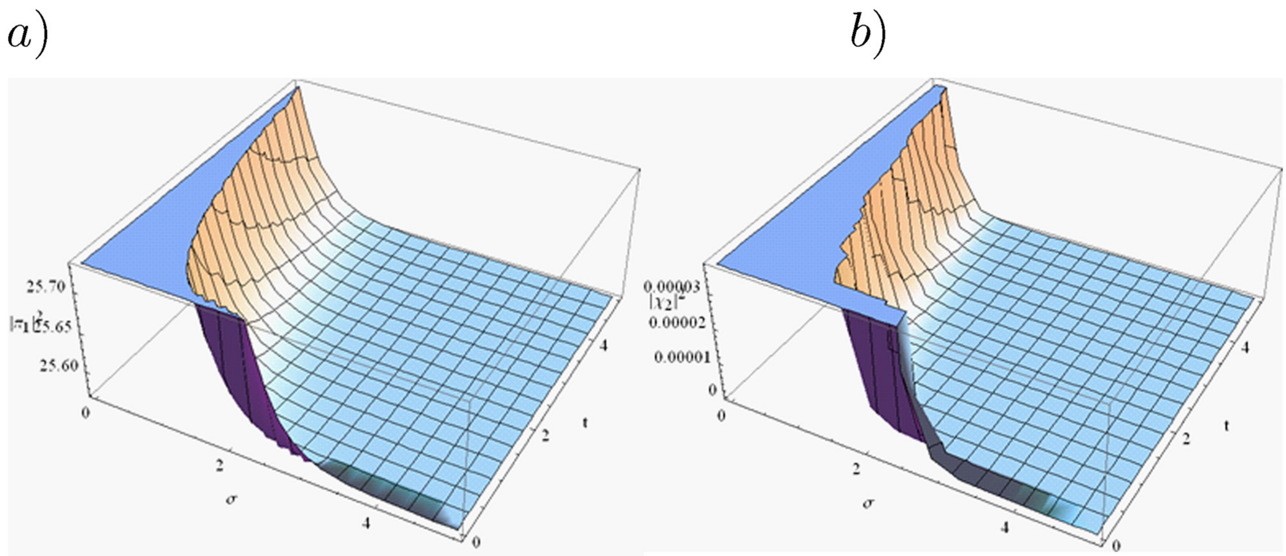

Figure 5: The magnetic flow graphics for the analytical solutions of the fractional (4.1) equations ($h = -2$, $\zeta = 1$, $\varpi = 0$) (a) $\pi_{15}(\sigma, t)$, (b) $\chi_{25}(\sigma, t)$.

5 Results and discussion

The magnetic flow graphics of the performed solutions are demonstrated in the illustrates by applying Mathematica. Also, we have obtained particle spherical tracing algorithm by spherical images with magnetic flow graphics. In Figures 4 and 5, we produce some numerical simulations of $\pi_{11}(\sigma, t)$ and $\pi_{15}(\sigma, t)$ in 3D plots when $0 \le \sigma \le 5$ and $0 \le t \le 5$. We displayed some of the solutions recovered for the presented fractional (4.1) equations by conformable derivative operator. Besides we showed 3D graphics for some of the solutions in Figures 4 and 5. Figures 4 and 5 were drawn for $A = 2.7$, $\chi_1 = 1.2$, $\eta = 0.3$, $\Delta = \Omega = 1$.

6 Conclusion

Spherical geometric models that illustrate a relativistic spherical magnetic particle can be organized by using geometrical potential associated with embedding of spherical particle worldline in de Sitter space $\mathbb{S}_1^2$ as framework density for action. In this investigation, we consider theory of magnetic spherical antiferromagnetic spin of spherical magnetic flows of Υ-magnetic particle with spherical Sitter frame in $\mathbb{S}_1^2$. Thus, extended direct algebraic method is defined to find soliton solutions of fractional (4.1) equation in $\mathbb{S}_1^2$. There are extreme many partial differential equations proceeding in mathematical physics and engineering modeling applications [46–48].

On the other hand, it can be expressed that the suggested approach is applicable to investigate various illustrations based on engineering and science [49–54].

The discussion of spherical electromagnetic forces and optical antiferromagnetic density is immensely straightforward and many remarkable investigations, review papers, and dissertations have been dedicated to these fields for a long time.

In our future papers under this study, we propose to present spherical inextensible flows of timelike particles in Minkowski spacetime. Also, we will further examine solitonic management of spherical magnetic vortex lines and management of electric vortex lines and their features of motions.

Acknowledgements: Bandar Almohsen is supported by Researchers Supporting Project number (RSP-2021/158), King Saud University, Riyadh, Saudi Arabia.

Funding information: This study was funded by National Natural Science Foundation of China (No. 71601072) and Key Scientific Research Project of Higher Education Institutions in Henan Province of China (No. 20B110006).

Author contributions: All authors have accepted responsibility for the entire content of this manuscript and approved its submission.

Conflict of interest: The authors state no conflict of interest.

References

[1] Smith AM. Polarization and magnetooptic properties of single-mode optical fiber. Appl Opt. 1978;17:52.
[2] Ross JN. The rotation of the polarization in low birefringence monomode optical fibres due to geometric effects. Opt Quantum Electron. 1984;16:455.
[3] Tomita A, Chiao RY. Observation of Berry's topological phase by use of an optical fiber. Phys Rev Lett. 1986;57:937.
[4] Chiao RY, Wu YS. Manifestations of Berry's topological phase for the photon. Phys Rev Lett. 1986;57:933.
[5] Haldane FDM. Path dependence of the geometric rotation of polarization in optical fibers. Optics Lett. 1986;11:730.
[6] Körpınar T, Demirkol RC. Electromagnetic curves of the linearly polarized light wave along an optical fiber in a 3D semi-Riemannian manifold. J Mod Optics. 2019;66:857.
[7] Körpınar T, Demirkol RC, Körpıinar Z. Soliton propagation of electromagnetic field vectors of polarized light ray traveling in a coiled optical fiber in Minkowski space with Bishop equations. Eur Phys J D. 2019;73:203.
[8] Körpınar T, Demirkol RC, Körpınar Z. Soliton propagation of electromagnetic field vectors of polarized light ray traveling in a coiled optical fiber in the ordinary space. Int J Geom Methods M. 2019;16:1950117.
[9] Körpınar T, Demirkol RC, Körpınar Z. Soliton propagation of electromagnetic field vectors of polarized light ray traveling along with coiled optical fiber on the unit 2-sphere S^2. Rev Mex Fis. 2019;65:626.
[10] Körpınar T, Demirkol RC. Electromagnetic curves of the linearly polarized light wave along an optical fiber in a 3D Riemannian manifold with Bishop equations. Optik. 2020;200:163334.
[11] Lamb GL. Solitons on moving space curves. J Math Phys. 1977;18:1654.
[12] Murugesh S, Balakrishnan R. Geometric characterizations of the Lamb equation. Phys Lett A. 2001;290:81.
[13] Berrry MV. Quantal phase factors accompanying adiabatic changes. Proc R Soc Lond A Math Phys Sci. 1984;392:45.
[14] Fang XS, Lin ZQ. Field in single-mode helically-wound optical fibers. IEEE Trans Microwave Theory Tech MTT 1985;33:1150.
[15] Ross JN. The rotation of the polarization in low birefringence monomode optical fibres due to geometric effects. Opt Quantum Electron. 1984;16:455.
[16] Kwiat PG, Chiao RY. Observation of a nonclassical Berry's phase for the photon. Phys Rev Lett. 1991;66:588.
[17] Wassmann F, Ankiewicz A. Berry's phase analysis of polarization rotation in helicoidal fibers. Applied Optics. 1998;37:18.
[18] Balakrishnan R, Bishop R, Dandoloff R. Geometric phase in the classical continuous antiferromagnetic Heisenberg spin chain. Phys Rev Lett. 1990;64:2107.
[19] Balakrishnan R, Bishop R, Dandoloff R. Anholonomy of a moving space curve and applications to classical magnetic chains. Phys Rev B. 1993;47:3108.
[20] Balakrishnan R, Dandoloff R. The Schrödinger equation as a moving curve. Phys Lett A. 1999;260:62.
[21] Körpınar T. New characterization of b-m_2 developable surfaces. Acta Scientiarum Technol. 2015;37:245.
[22] Körpınar T, Demirkol RC. Frictional magnetic curves in 3D Riemannian manifolds. Int J Geom Methods Mod Phys. 2018;15:1850020.
[23] Körpınar T, Demirkol RC. Gravitational magnetic curves on 3D Riemannian manifolds. Int J Geom Methods Mod Phys. 2018;15:1850184.
[24] Podlubny I. Fractional differential equations. San Diego: Academic Press; 1998.
[25] Kilbas AA, Srivastava HM, Trujillo JJ. Theory and applications of fractional differential equations. Amsterdam: Elsevier; 2006.
[26] Sabatier J, Agrawal OP, Machado JAT. Advances in fractional calculus. Dordrecht: Springer; 2007.
[27] Mainardi F. Fractional calculus and waves in linear viscoelasticity: an introduction to mathematical models. Singapore: World Scientific; 2010.
[28] Yang X-J. General fractional derivatives: theory, methods and applications. New York: CRC Press; 2019.
[29] Khalil R, AlHorani M, Yousef A, Sababheh M. A new definition of fractional derivative. J Comput Appl Math. 2014;264:65.
[30] Eslami M, Rezazadeh H. The first integral method for Wu-Zhang system with conformable time-fractional derivative. Calcolo. 2016;53:475.
[31] Çenesiz Y, Baleanu D, Kurt A, Tasbozan O. New exact solutions of Burgers' type equations with conformable derivative. Waves Random Complex Media. 2017;27:103.
[32] Eslami M, Khodadad FS, Nazari F, Rezazadeh H. The first integral method applied to the Bogoyavlenskii equations by means of conformable fractional derivative. Opt Quant Electron. 2017;49:391.
[33] Caputo M. Linear models of dissipation whose Q is almost frequency independent: part II. Geophys J Int. 1967;13:529.
[34] Baleanu D, Golmankhaneh AK, Baleanu MC. Fractional electromagnetic equations using fractional forms. Int J Theoret Phys. 2009;48(11):3114.
[35] Klimek K. Fractional sequential mechanics-models with symmetric fractional derivative. Czech J Phys. 2005;55:1447–53.
[36] Laskin N. Fractional quantum mechanics. Phys Rev E. 2000;62:3135.
[37] SG, Samko, AA, Kilbas, OI, Marichev. Fractional integrals and derivatives theory and applications. New York: Gordon and Breach; 1993.
[38] Al-Smadi M, Freihat A, Khalil H, Momani S, Khan RA. Numerical multistep approach for solving fractional partial differential equations. Int J Comput Meth. 2017;14:1750029.
[39] Al-Smadi M, Arqub OA, Momani S. Numerical computations of coupled fractional resonant Schrödinger equations arising in quantum mechanics under conformable fractional derivative sense. Physica Scripta. 2020;95(7):075218.
[40] Al-Smadi M, Arqub OA. Computational algorithm for solving fredholm time-fractional partial integrodifferential equations of Dirichlet functions type with error estimates. Appl Math Comput. 2019;342:280–94.
[41] Al-Smadi M, Arqub OA, Hadid S. An attractive analytical technique for coupled system of fractional partial differential

equations in shallow water waves with conformable derivative. Commun Theoret Phys. 2020;72(8):085001.
[42] Al-Smadi M, Arqub OA, Zeidan D. Fuzzy fractional differential equations under the Mittag-Leffler kernel differential operator of the ABC approach: theorems and applications. Chaos Soliton Fractal. 2021;146:110891.
[43] Yavuz M, Yokus A. Analytical and numerical approaches to nerve impulse model of fractional-order. Numer Meth Partial Differ Equ. 2020;36(6):1348.
[44] Yavuz M, Novel solution methods for initial boundary value problems of fractional order with conformable differentiation. Int J Optim Control Theories Appl (IJOCTA). 2018;8(1):1.
[45] Yavuz M, Yaşkıran B. Conformable derivative operator in modelling neuronal dynamics. Applications Applied Math. 2018;13(2):803.
[46] Yavuz M, Yaşkıran B, Approximate-analytical solutions of cable equation using conformable fractional operator. New Trends Mathe Sci. 2017;5(4):209.
[47] Naik PA, Yavuz M, Qureshi S, Zu J, Townley S. Modeling and analysis of COVID-19 epidemics with treatment in fractional derivatives using real data from Pakistan. European Phys J Plus. 2020;135(10):1–42.
[48] Yavuz M, Sene N. Stability analysis and numerical computation of the fractional predator-prey model with the harvesting rate. Fractal Fractional. 2020;4(3):35.
[49] Körpinar T. Optical directional binormal magnetic flows with geometric phase: Heisenberg ferromagnetic model. Optik. 2020;219:165134.
[50] Körpınar T, Demirkol RC, Körpınar Z. Approximate solutions for the inextensible Heisenberg antiferromagnetic flow and solitonic magnetic flux surfaces in the normal direction in Minkowski space. Optik. 2021;238:166403.
[51] Körpınar T, Demirkol RC, Körpınar Z. Binormal schrodinger system of wave propagation field of light radiate in the normal direction with q-HATM approach. Optik. 2021;235:166444.
[52] Körpınar T, Demirkol RC, Körpınar Z. Polarization of propagated light with optical solitons along the fiber in de-sitter space $\mathbb{S}_1^2$. Optik. 2021;226:165872.
[53] Körpinar T. New Heisenberg antiferromagnetic spin for quasi normal magnetic flows with geometric phase. Int J Geom Methods Mod Phys. 2021;18:2150061.
[54] Körpınar T, Demirkol RC, Asil V. Elastic magnetic curves of ferromagnetic and superparamagnetic models on the surface. Int J Geom Methods Mod Phys. 2021;18:2150037.